Spatially Varying Energy Gap in the CuO Chains of $YBa_2Cu_3O_{7-x}$ Detected by Scanning Tunneling Spectroscopy

H. L. Edwards,* D. J. Derro, A. L. Barr, J. T. Markert, and A. L. de Lozanne†
Department of Physics, The University of Texas at Austin, Austin, Texas 78712-1081
(Received 26 April 1995)

Current-imaging tunneling spectroscopy (CITS) was performed on cold-cleaved single crystals of $YBa_2Cu_3O_{7-x}$ at 20 K. CITS data include $I(V)$ curves taken simultaneously with a topographic scanning tunneling microscopic image. $I(V)$ curves taken on CuO chains show an energy gap of about 20 meV which disappears near oxygen vacancies. We explain several features of large-junction $I(V)$ measurements, photoemission spectroscopy, and single-point $I(V)$ spectroscopy in terms of local effects detected by our CITS measurements. Finally, we consider the possibilities that this energy gap is due to either a charge-density wave or proximity-coupled superconductivity from the CuO_2 planes.

PACS numbers: 74.72.Bk, 61.16.Ch, 68.35.Bs, 74.50.+r

The superconductivity in the copper-oxide high-temperature superconductors (HTSC) is generally thought to occur in the CuO_2 planes, with the rest of the material layers serving only structural or charge-balance functions. $YBa_2Cu_3O_{7-x}$ (YBCO) is a HTSC with a special feature interleaved between its CuO_2 planes: the CuO chains. These one-dimensional structures give rise to partially filled energy bands, allowing the possibility of metallic one-dimensional electronic states. Recently, far-infrared spectroscopy detected a superfluid component in the CuO chains [1]. This is consistent with superconductivity induced in the CuO chains by the proximity effect with the superconducting CuO_2 planes [1].

The electronic structure of the CuO chains is important for three reasons. First, metallic CuO chains have their own electronic, magnetic, and transport signatures, which complicate the interpretation of measurements of superconductivity in the CuO_2 planes. Second, the presence of metallic chains interleaved between the superconducting CuO_2 planes may modify the superconducting behavior of the CuO_2 planes. Finally, the properties of a one-dimensional metal near a two-dimensional superconductor are interesting in their own right. This Letter focuses on the last topic.

In previous work, we used a scanning tunneling microscope (STM) to measure $I(V)$ curves, which displayed an energy gap of $2\Delta/kT_c = 6$–8 in YBCO [2]. Although we obtained atomic-resolution images of the CuO chains, we were unable to identify the $I(V)$ curves uniquely with any crystallographic features. More recently, we have observed electronic modulations along the CuO chains with wavelength and reversed-bias behavior consistent with a charge-density wave (CDW) [3,4]. In this Letter, we present the results of scanning tunneling spectroscopy (STS) measurements on YBCO that detect an energy gap in the CuO-chain states. This gap disappears near oxygen vacancies. We discuss the possibilities that this energy gap in the CuO chains is due to proximity-coupled superconductivity or a CDW.

To perform STM and STS on YBCO, we cleave the single crystals in ultrahigh vacuum at 20 K. The measurements are carried out immediately after cleaving, without warming the crystals [2]. We have previously seen several types of surface structure [2–4]. The most interesting structure is a chainlike feature with electronic modulations and depressions along its length [3]. The chains are separated by the **a**-direction lattice constant. Because the only one-dimensional feature of YBCO is the CuO chain, these chainlike images must be associated with the CuO chains.

The wavelength of the electronic modulations along chains is several times longer than the **b**-direction lattice constant, indicating that these features are not due to individual atoms. Furthermore, these modulations reverse sign under bias reversal—the empty states are 180° out of phase with the filled states. The wavelength and the reversed-bias behavior of these modulations are consistent with the hypothesis of a CDW in the CuO chains [4]. However, these observations do not provide a smoking gun: there are other phenomena of the Fermi-level electrons that should have the same characteristic wavelength and reversed-bias behavior.

The chain modulations are enhanced near the several-nm-long depressions in the chains. The areal density of these depressions matches that expected for oxygen vacancies in well-oxygenated YBCO crystals; we assert that each depression is associated with an oxygen vacancy [3]. In the data that we show below, it is near these depressions that the measured energy gap disappears.

Current-imaging tunneling spectroscopy (CITS) is now a fairly standard technique [5]. Our CITS data were taken on a $(128\ \text{pixel})^2$ grid with 32 different bias voltages, resulting in a three-dimensional data matrix with half a million elements. In order to obtain a high enough signal-to-noise ratio in our data (we need a noise level of <0.1 pA), we had to average the current readings 256 times. Thus, each CITS data set requires over 10^8 current measurements. This large amount of data was taken in under 2 hours using a fast computer (486/66) and a new Transputer-based electronics system, which ran the digital feedback for STM and performed some data averaging [6].

Figure 1 shows constant-current STM images taken (a) before, (b) during, and (c) after the CITS data. These images are 10 nm on a side, and they were taken at a sample bias voltage of +300 mV and a current of 200 pA. The voltage values labeling the CITS images in Fig. 1(d) refer to the sample bias. By comparing Figs. 1(a) and 1(c), we see that the thermal drift was very small over the 2-h imaging time; the same features appear in both images with only a slight shift. The similarity of Figs. 1(a) and 1(c) also indicates that the sample was not damaged or modified during CITS. Figure 1(b) shows the STM image obtained during CITS; because of the long imaging time, the tip underwent several changes while the CITS data was being taken. These tip changes should not affect the interpretation of our data as long as we compare $I(V)$ curves from the same horizontal band (i.e., with the same tip).

Figure 1(d) shows the CITS data, displayed as 32 images at different bias voltages. The negative-sample-bias images appear to have inverted contrast relative to the positive-sample-bias images. This is due to the sign change in the tunneling current when the bias voltage is reversed. In previous work, we have accounted for the sign change by displaying the negative-bias images in reversed contrast [3,4]. In this manner, images can be interpreted as the integrated density of states, allowing us to examine the relation between the empty and filled electronic states near the Fermi level in the CuO chains [3,4]. In this Letter, we display the data without reversed contrast because comparison is being made with $I(V)$ curves; reversing the contrast of some images would

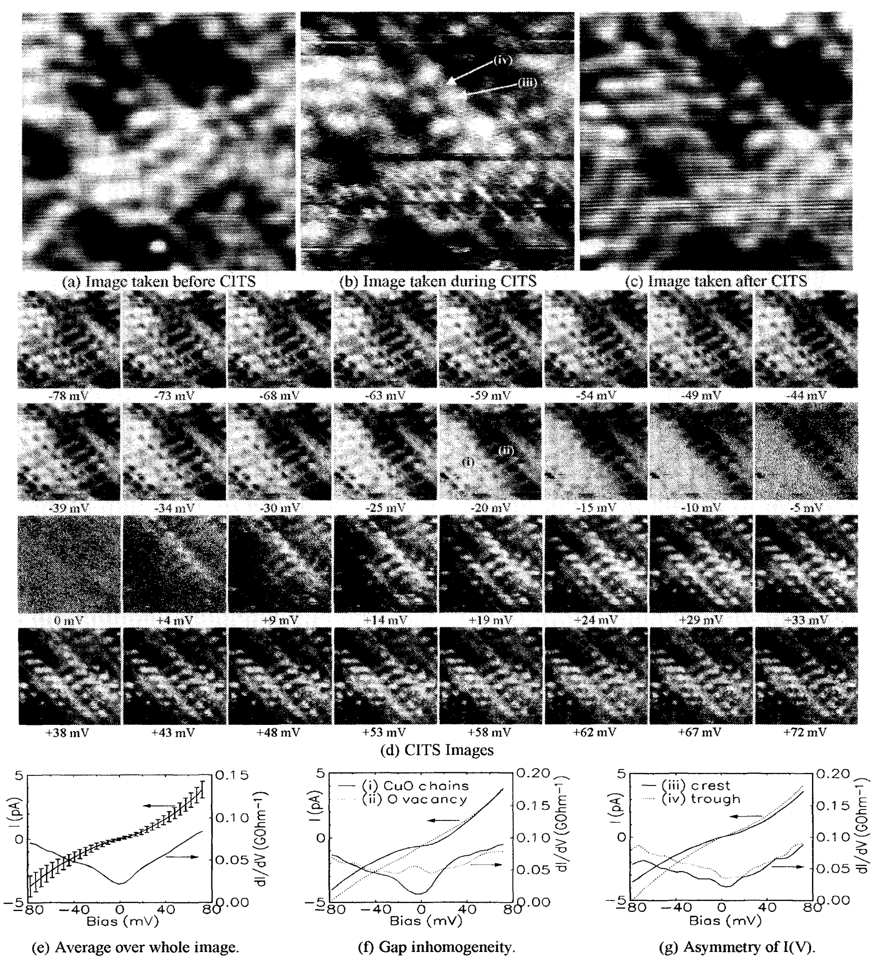

FIG. 1. Current-imaging tunneling spectroscopy (CITS) data on YBCO. (a) and (c) are $(10\ \mathrm{nm})^2$ images taken at +300 mV sample bias and 200 nA current (a) before and (c) after CITS. (b) Constant-current image (+300 mV sample bias, 200 nA current) taken during CITS. (d) CITS images show the onset of features at different energies. (e),(f) CITS data can be displayed as STS to examine the variation of $I(V)$ curves with topography.

obfuscate the correspondence between CITS images and $I(V)$ curves.

Several features can be seen directly from these images. First, the electronic modulations along the chains appear at different voltages. Where there is a heavy concentration of depressions (oxygen vacancies), the chains appear at ± 5 mV from the Fermi surface. Away from the depressions, the chain modulations do not appear until about 20 mV, indicating the presence of an energy gap in the spectrum that corresponds to these modulations. This is the essential result of our data: the energy gap on the chains is destroyed near oxygen vacancies.

Another way of viewing the CITS data is as a set of local $I(V)$ curves as in STS. We average the $I(V)$ curves over the entire image in Fig. 1(e). The error bars on $I(V)$ represent the computed standard deviation of this data set. Note that noise level, as given by the smoothness of the $I(V)$ curves, is much smaller than these error bars. The small magnitude of the error bars indicates that the $I(V)$ curves do not change too radically over the image.

We can compare our spatially averaged $I(V)$ curve of Fig. 1(e) to that obtained with macroscopic YBCO-Pb tunneling junctions by Gurvitch *et al.* [7]. The spectra of Gurvitch *et al.* show more structure than our $I(V)$ curve of Fig. 1(e). This may be due to high-frequency electrical noise in our bias voltage, which is provided by the same digital electronics box housing the high-voltage piezo amplifiers and some digital electronics [6]. Several features compare favorably, however. Both sets of data exhibit a linear conductance background above about 40 mV, a gaplike feature of about 20 mV, and a zero-bias conductance, which is about half of that just outside the gap. For a homogeneous superconductor, one would expect nearly no zero-bias conductance for temperatures well below T_c. Several of these features can be illuminated by looking at the local spectra.

Far from a depression [region marked (i) on the -20 mV image of Fig. 1(d)], the $I(V)$ curve [solid curve of Fig. 1(f)] displays a gap of roughly 20 mV, with a low zero-bias conductance. This agrees well with our single-point $I(V)$ spectra, which show an energy gap of 20–30 meV, giving a strong coupling value of $2\Delta/kT_c = 6$–8 if this energy gap is associated with superconductivity [2]. In the neighborhood [marked (ii) on the -20 mV image of Fig. 1(d)] of a depression along a CuO chain, we obtain the $I(V)$ curve [dotted curve of Fig. 1(f)], which is roughly linear through zero bias, indicating the lack of an energy gap in the spectrum. Note that the gap in this curve is filled in by adding spectral weight inside the gap; in this curve, a peak in the conductance at zero bias resulted. This feature has been seen by other authors; we intend to analyze the behavior of this peak in different locations in future work to help identify its origin. One point where our new CITS data and our old single-point $I(V)$ data diverge is on the energy resolution: our old analog electronics seemed to have less noise in the bias voltage, resulting in less-smeared conductance peaks in dI/dV and even lower zero-bias conductance [2].

In the context of this spatial variation, the high zero-bias conductance of Gurvitch *et al.* and our Fig. 1(e) is seen to be the result of averaging gapped and nongapped regions of the CuO chain layer. Although the microscopic structure of the junctions of Gurvitch *et al.* was not known, it is plausible that inhomogeneities in the energy gap caused a metallic component to the tunneling. Note that we did not need to invoke tunneling through step edges to arrive at this conclusion.

Another common feature of $I(V)$ spectra obtained on YBCO is asymmetry about zero bias. The $I(V)$ curve of a tunneling junction between a normal metal electrode and a BCS superconducting electrode should be essentially symmetrical. However, there are numerous reports of asymmetric $I(V)$ curves on YBCO in the literature [8]. The reversed-bias images in our earlier work [3] indicated that this may be due to the alternating empty- and filled-state maxima along the chains. Our new data allow us to make this assignation more directly.

According to the reversed-bias behavior we observed previously [3], an empty-state minimum should correspond to a filled-state maximum and vice versa. This alternation of filled- and empty-state maxima is reflected in the asymmetry of the $I(V)$ curves in our CITS data. In Fig. 1(g), we show $I(V)$ curves taken from an empty-state crest (solid line) and an empty-state trough (dotted line). Specifically, we located a crest (iii) and a trough (iv) along a CuO chain in the topographic image of Fig. 1(b) and averaged several nearest-neighbor $I(V)$ curves to eliminate noise. Although the effect is not drastic, we see that on the empty-state crest the conductance is stronger at positive sample biases (electrons tunneling from filled states in the tip to empty states in the sample). On the filled-state crest (empty-state trough), the conductance is stronger at negative sample bias voltages (electrons tunneling from filled states in the sample to empty states in the tip). It should be noted that the overall conductance of all $I(V)$ curves is fixed by the imaging conditions set for Fig. 1(b) (+300 mV and 200 nA). Our CITS data thus identify one source of $I(V)$-curve asymmetry: the spatial offset of empty and filled states along the CuO chains.

These CITS results also offer a potential explanation of why photoemission on YBCO has failed to see an energy gap, even on cold-cleaved crystals [9]. Photoemission averages over a large area, so a given data set must contain contributions from solid (gapped) chains and (metallic) oxygen vacancy sites. In order to measure an energy gap, one relies upon an absence of signal; since the chains near the oxygen vacancies have no gap, they will produce a signal which will obscure the gap that does occur elsewhere.

Because the superconductivity in copper-oxide HTSC occurs mainly in the CuO_2 planes, the interpretation of a gap in the CuO chains is not entirely straightforward. We offer two possibilities: proximity-coupled superconductivity or CDW in the CuO chains. Because the CuO chains reside less than 1 nm from the CuO_2 planes, it is conceivable that the chains superconduct due to the proximity effect with the CuO_2 planes. This assertion was made to interpret the observation of an excess superfluid density in the **b** direction of YBCO [1]. In this picture, the energy gap that we have observed in the CuO chains corresponds to superconductivity; the large magnitude of the gap indicates that the proximity coupling is strong. The disappearance of the energy gap near the oxygen vacancies can be understood as well. An oxygen vacancy acts as a magnetic scattering center for CuO chain electrons [10], causing pair breaking and hence gap destruction.

An alternative explanation that we have considered before is that the CuO chains participate in a CDW state. This scenario is plausible because any one-dimensional metal is prone to such a state [11]. Our previous data—the modulations' wavelength and reversed-bias behavior—are consistent with this hypothesis. Our new data prompt a closer examination of this scenario. There are two types of CDW that may be present in the CuO chains: static and dynamic. If the CuO chains support a static CDW, then the modulations that are strongest near the oxygen vacancies correspond to the CDW wave function; hence the CDW gap should be strongest near the oxygen vacancies. This contradicts our CITS data.

The other possibility—a dynamic CDW—can be explained within the context of our data as follows. In a dynamic CDW, the corrugations slide along the CuO chains until they hit a defect that may pin them locally. If this is the case, the strong modulations are caused by the dynamic CDW pinned at the oxygen vacancies, and the modulations die off as a function of distance from the pinning site, as is observed in most of our images. If this pinning is strong enough, it may serve to interrupt the CDW gap. It is not currently known whether the gap is interrupted near a strong CDW pinning site. This issue may be addressed by performing CITS measurements on a standard CDW material such as $NbSe_2$ or TaS_2.

It might be argued that this represents only a surface effect since these modulations have not been observed in the bulk. A fast Fourier transform of our STM images shows satellites due to the CuO-chain modulations [4]; why would x-ray or neutron diffraction miss these features? First, it is difficult to obtain large enough untwinned crystals of YBCO to obtain good statistics in these bulk measurements. In addition, oxygen vacancies are distributed randomly throughout the crystal so that there is no long-range coherence to reinforce the signal. Although one can see some chain-to-chain correlation in our STM images [2–4], this correlation does not extend more than a few nm perpendicular to the chains and is not enough to allow a strong bulk measurement. The coherence along the chains is only a few nm as well, since the modulations are strongest in the depressions and decay away from them. Thus, it would be difficult for standard diffraction techniques to find these modulations.

There are other ways of detecting the local behavior of the chain electrons. For instance, neutron scattering data may be analyzed in terms of pair-distribution functions to explore the correlations between the motions of neighboring ions [12]. Single-crystal NMR measurements of T_2 for the CuO-chain Cu moments may give some information about the distribution of local interactions in the CuO chains as well.

In conclusion, we have observed an energy gap in the CuO chains whose magnitude of 20 meV is in agreement with the values measured in our earlier work [2] and in the literature [8]. Using CITS, we find that this energy gap disappears near oxygen vacancies. This result is consistent with either proximity-coupled superconductivity in the CuO chains or a CDW state in the one-dimensional CuO chains.

We acknowledge useful discussions with Zhenxi Dai and support from the Texas Advanced Technology/Research Program (Grant No. 3658-172), R. A. Welch Foundation (Grants No. F-1047 and No. F-1191), and the National Science Foundation (Grant No. DMR-9158089).

*Present address: Texas Instruments, Inc., MS 147, P.O. Box 655936, Dallas, TX 75265.

†To whom all correspondence should be addressed. Electronic address: lozanne@physics.utexas.edu

[1] D. N. Basov *et al.,* Phys. Rev. Lett. **74**, 598 (1995).
[2] H. L. Edwards, J. T. Markert, and A. L. de Lozanne, Phys. Rev. Lett. **69**, 2967 (1992).
[3] H. L. Edwards, J. T. Markert, and A. L. de Lozanne, J. Vac. Sci. Technol. B **12**, 1886 (1994).
[4] H. L. Edwards, A. L. Barr, J. T. Markert, and A. L. de Lozanne, Phys. Rev. Lett. **73**, 1154 (1994).
[5] See, for instance, A. W. Munz, Ch. Zeigler, and W. Göpel, Phys. Rev. Lett. **74**, 2244 (1995).
[6] TOPSystem II SPM control electronics, manufactured by WA Technologies (Cambridge, U. K.).
[7] M. Gurvitch *et al.,* Phys. Rev. Lett. **63**, 1008 (1989).
[8] T. Hasegawa, H. Ikuta, and K. Kitazawa, in *Physical Properties of High Temperature Superconductors III,* edited by D. M. Ginsberg (World Scientific, Singapore, 1992).
[9] M. Lindroos *et al.,* Physica (Amsterdam) **212C**, 347 (1993).
[10] V. Z. Kresin and S. A. Wolf, Phys. Rev. B (to be published).
[11] A. W. Overhauser, Adv. Phys. **12**, 843 (1978).
[12] T. Egami *et al.,* in Proceedings of the OE/LASE '94 Conference, SPIE, Los Angeles, 1994.

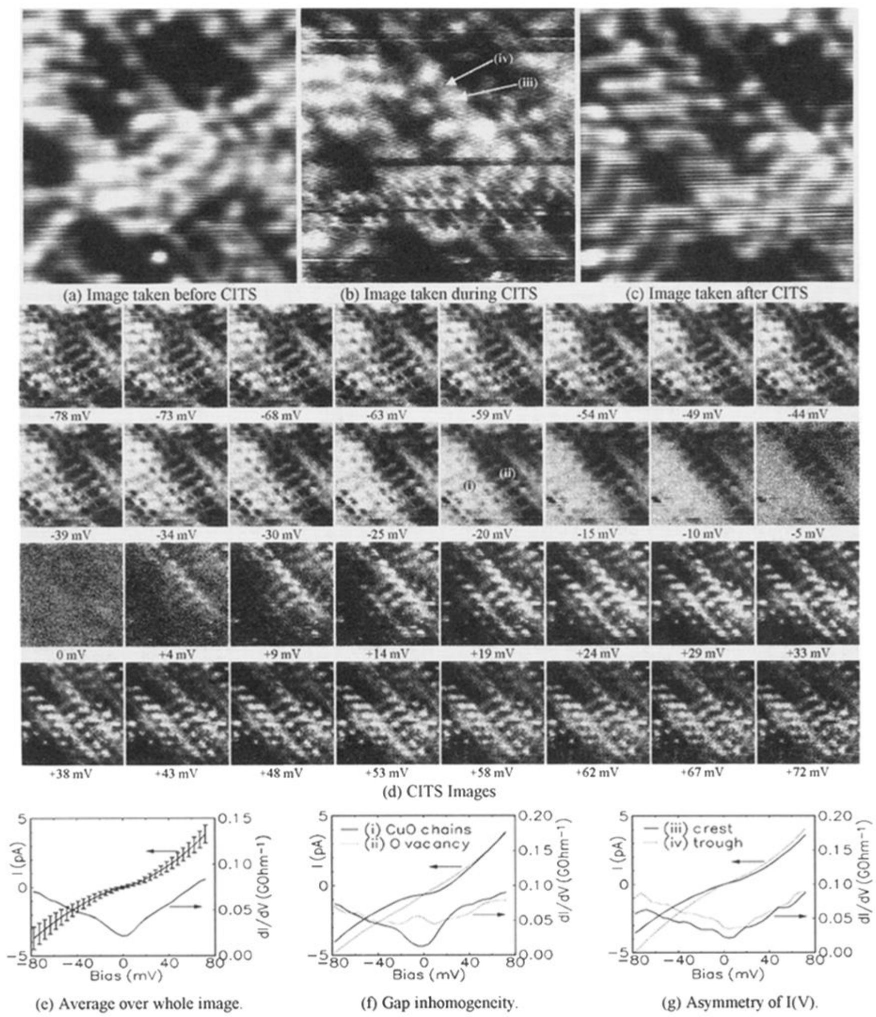

FIG. 1. Current-imaging tunneling spectroscopy (CITS) data on YBCO. (a) and (c) are $(10\ \mathrm{nm})^2$ images taken at $+300$ mV sample bias and 200 nA current (a) before and (c) after CITS. (b) Constant-current image ($+300$ mV sample bias, 200 nA current) taken during CITS. (d) CITS images show the onset of features at different energies. (e),(f) CITS data can be displayed as STS to examine the variation of $I(V)$ curves with topography.